



Antimicrobial Effects of Tannic and Gallic Acids: A Study on 3D-Printed Polylactic Acid Surfaces Against *P. aeruginosa* and *S. aureus*

Badr Errabiti, Amal El Aabedy*, Sara Er-Rahmani, Soumya El Abed, Saad I. Koraichi

Laboratory of Microbial Biotechnology and Bioactive Molecules, Faculty of Science and Technology, Sidi Mohamed Ben Abdellah University, Fez, Morocco.

ARTICLE INFO

Article history:

Received 24 April 2024

Revised 04 June 2024

Accepted 08 October 2024

Published online 01 November 2024

ABSTRACT

3D printing materials, such as polylactic acid (PLA), are widely used in the medical industry; however, their limited antibacterial properties make them susceptible to microbial adhesion and biofilm formation, potentially leading to significant health risks. This study investigates the potential of tannic acid (TA) and gallic acid (GA) to enhance PLA's antibacterial efficacy and surface properties. The aim was to assess the effects of TA and GA on the hydrophobicity, surface tension, and electron donor/acceptor properties of PLA. Contact angle measurements were used to evaluate these physicochemical properties on untreated and treated PLA surfaces. The antibacterial activity of TA and GA against *Pseudomonas aeruginosa* and *Staphylococcus aureus* was tested, and the DLVO (Derjaguin-Landau-Verwey-Overbeek) theory was applied to calculate the total free energy of bacterial adhesion. Scanning electron microscopy (SEM) was employed to observe bacterial adherence. The untreated PLA was initially hydrophobic with a strong electron donor property. Following TA and GA treatments, the PLA surface became hydrophilic and displayed increased electron donor characteristics, except in the MICGA/S (minimum inhibitory concentration of GA vs. *S. aureus*) group. Post-treatment, the adhesion free energies for both bacterial strains generally increased, indicating lower bacterial adherence. SEM imaging confirmed a reduction in bacterial attachment across treatments, with the MICGA/P (GA vs. *P. aeruginosa*) treatment achieving 100% inhibition. The study concludes that the integration of TA and GA into PLA surfaces significantly improves antibacterial and surface properties, enhancing their suitability for biomedical applications requiring bacterial resistance.

Copyright: © 2024 Errabiti *et al.* This is an open-access article distributed under the terms of the [Creative Commons Attribution License](https://creativecommons.org/licenses/by/4.0/), which permits unrestricted use, distribution, and reproduction in any medium, provided the original author and source are credited.

Keywords: Tannic acid, Gallic acid, Adhesion, PLA.

Introduction

Nosocomial infections are illnesses acquired either within 48 hours of admission or up to three days following discharge.¹ These infections can arise in different environments, such as hospitals, long-term care facilities, and outpatient settings. Healthcare-associated infections also include occupational infections, which may affect healthcare workers.² In past years, the incidence of infection in hospitals in Europe reached an infection ratio of 1/10 patients and a fatality rate of 5000 people per year.³ A patient with a nosocomial illness spends 2.5 times as much time in the hospital, increasing the likelihood of infections; this is particularly relevant given that bacterial biofilms account for approximately 65% of all bacterial infections, suggesting they are a significant factor in the development of nosocomial infections.⁴ Apparently, microbial adhesion is the initial step in the formation of a biofilm.⁵ The attachment phase is controlled by physical and/or chemical interactions between the free-living cell and the substratum.⁶ Likewise, the Derjaguin-Landau-Verwey-Overbeek (DLVO) theory, which considers hydrophobicity/hydration effect, electrostatic interactions, and the thermodynamic viewpoint, is a measurement of bacteria-substratum adhesion.⁷

*Corresponding author. E mail: amal.elaabedy@usmba.ac.ma

Tel: [+05 35 60 96 60/61](tel:+053560966061)

Citation: Errabiti B, El Aabedy A, Er-Rahmani S, El Abed S, Koraichi SI. Antimicrobial Effects of Tannic and Gallic Acids: A Study on 3D-Printed Polylactic Acid Surfaces Against *P. aeruginosa* and *S. aureus*. Trop J Nat Prod Res. 2024; 8(10): 8753 – 8763 <https://doi.org/10.26538/tjnpr/v8i10.18>

Official Journal of Natural Product Research Group, Faculty of Pharmacy, University of Benin, Benin City, Nigeria
Therefore, to avoid bacterial adherence, it is necessary to clean and disinfect the surfaces of materials used in hospitals. Numerous

investigations, such as that of Dong *et al.*⁸ have shown that tannic acid (TA) is a potent inhibitor of bacterium adhesion and colonisation in *S. aureus*, *E. coli*, and *P. aeruginosa* for biomedical applications, thus constituting a viable method for contamination by these bacteria. In turn, it has been shown that chitosan films containing gallic acid (GA) have substantial antibacterial activity against *E. coli*.⁹ TA acid and GA are the main constituents of a variety of therapeutic plants.^{10,11} According to reports, TA and GA have antibacterial effects against a range of bacteria, including *Pseudomonas aeruginosa*, *Staphylococcus aureus*, *Escherichia coli*, *Enterococcus faecalis*, and *Streptococcus pyogenes*.¹²⁻¹⁴ TA has been employed as a single precursor for the deposition of coatings on substrate surfaces, demonstrating the inhibition of *E. coli* and *S. aureus* adhesion, as well as the development of *S. aureus* biofilms.¹⁵ Furthermore, GA has been identified as a powerful antibacterial agent against *S. aureus* in another investigation.¹⁶ GA may be utilised as gallic acid-functionalised gauze, which exhibits antiadhesion properties against *E. coli*, *S. aureus*, and MRSA.¹⁷ Through its capacity to open up numerous possibilities in various sectors, 3D printing technology emerges as a unique technology.¹⁸ It can create actual materials based on the sequential addition of constituents in a dimensional image.¹⁹ Until recently, 3D printing engineering has proven effective in medicinal applications.²⁰ It helps lower fabrication costs by enabling significant advancements in medical tools and facilities, such as the customisation of devices for individual patients, rapid prototyping of innovative designs, and the production of complex geometries that traditional methods cannot achieve.²¹ Additionally, the precision of 3D printers is rapidly advancing, and high-resolution models are now more affordable for desktop use. A standard extruder printer typically operates with a 200 µm gap between layers, and the printing process naturally results in surface roughness for all polymers.²¹ These textured surfaces can create an optimal setting for initial bacteria attachment, leading to the subsequent development of biofilms.²² The research methods employed, including contact angle

measurements and SEM analysis, are highly relevant for understanding surface interactions and bacterial adhesion. These methods provide detailed insights into the changes in hydrophobicity, surface tension attributes, and electron donor and acceptor characteristics of the PLA surfaces. The innovation in this research is attributed to enhancing the antibacterial properties of PLA using natural compounds. By integrating TA and GA into PLA surfaces, we propose a new strategy for developing advanced materials for biomedical applications. This approach could greatly enhance the performance and safety of medical devices and equipment, addressing a critical need in healthcare for materials that resist bacterial colonisation and infection.

This study pioneers an uncharted realm of research by investigating the antiadhesion properties of natural compounds, specifically tannic and gallic acid, on the widely employed polylactic acid (PLA) 3D printing material. Notably, this research represents the first of its kind, with no prior studies exploring the antiadhesion potential of these natural chemicals on PLA. Our work introduces a novel dimension to the field of materials science and medical technology, offering fresh perspectives that hold great promise for enhancing healthcare equipment and device performance. Therefore, the current work investigated the impact of antibacterial compounds TA and GA on the physicochemical features of 3D-printed PLA, as well as their antiadhesion effectiveness against *P. aeruginosa* and *S. aureus* (major causes of nosocomial infections,^{23, 24}) on PLA, using SEM analysis.

Materials and Methods

Chemical standards: Tannic acid (TA) and Gallic acid (GA) were of analytical grade with 99.5% purity acquired from Sigma-Aldrich. TA and GA were dissolved in dimethylsulfoxide (DMSO 2%) at a concentration of 1 mg/mL.

Strains bacteria inoculum preparation: *Staphylococcus aureus* CIP543154 purchased from the Collection of Institut Pasteur (Paris, France), and *Pseudomonas aeruginosa* ATCC27653 obtained from the American Type Culture Collection (Manassas, VA, USA) were the microorganisms employed in this investigation.

Antibacterial activity of Tannic acid and Gallic acid

In a test tube containing saline 0.9%, the solutions of test strains were normalised according to the Mac Farland 0.5 range, or around 1.5×10^8 Colony Forming Units (CFU/mL). The bacterial sample was diluted further with anaerobic broth to provide a final inoculum of 10^6 CFU/mL.

Minimum Inhibitory Concentration (MIC) Determination

50 μ L of TA and GA were serially diluted and added to 96-well plates containing 50 μ L of LB broth, as described by CLSI M31-A3.²⁵ The concentration ranged from 5 to 0.0097 mg/mL. Each well of the microdilution plate was inoculated with 50 μ L (10^6 CFU.mL⁻¹) of inoculum and incubated for 24 hours at 37°C. Once the incubation was complete, 15 μ L of resazurin (0.015 %) was added to the wells and incubated for 2 hours to see the colour changes. In comparison to the positive control (broth and strain only), the MIC was defined as the lowest compound concentration at which no growth was observed. All of the tests were carried out in triplicates. The average results were determined after each test was completed in triplicate.

Surface characterization

PLA Material preparation

The fused deposition modelling (FDM) 3D printing method was utilised in this study. PLA material was produced using a 3D printer from Ultimaker (Utrecht, Netherlands) with the following settings: 200°C for the nozzle, 60°C for the bed temperature, 0.1 mm for the layer height, and +/- 45° for the raster angle. PLA components were created using the Autodesk Fusion 360 program (Autodesk, San Francisco, California, USA). Using the Ultimaker Cura program (Ultimaker, Utrecht, Netherlands), the PLA parts file was transformed from an STL file to a print file (GCODE file). Layers were sliced to a thickness of 0.1 mm. A spool of PLA filament was placed into the printer. The filament was fed through the extrusion head and nozzle as soon as the

nozzle heated up to 200 °C. The printer deposits the melted material in layers along the designated path by extruding it into thin strands. The material cools and solidifies after being placed. After printing, the material was chopped into pieces of length = 1 cm, width = 1 cm and thickness = 0.5 cm. The pieces were disinfected by soaking them in a 95% ethanol solution for 10 minutes, followed by three rinses with distilled water, and then left to air dry.

Surface roughness

The surface roughness of the printed samples was evaluated using a profilometer (SurfTest SJ-310, tip radius 2 μ m, load 0.75 mN, Mitutoyo Corporation, Kawasaki, Japan). Five measurements were taken of the printed samples (stylus speed: 0.5 mm s⁻¹, assessment length: 0.8 mm) from the midpoint at various distances and orientations. The stylus was regularly advanced and retracted along the same path five times for each evaluation. The observations were screened using a 0.8 mm cut-off (Λ_c) value (Gauss profile filter).

Contact angle measurements

The contact angle was calculated as the angle formed by the solid-liquid interfaces crossing at the atmosphere-liquid-solid point.²⁶ The sessile drop technique is based on goniometer equipment (GBX, instruments, France). Three liquids are required for this procedure.²⁷ Two polar liquids (Water and Formamide) and one apolar liquid (Diodomethane) are described by their specific surface tensions (Table 1). According to the technique outlined by Sadiki *et al.*²⁸ measurements were made on the bacterial lawn that had been deposited on filter membranes in the case of bacterial cells. Essentially, by filtering the suspension under negative pressure, the bacterial cells contained in the sterile KNO₃ solution were deposited on a cellulose acetate membrane filter (0.45 m). The membrane filter created a layer of cells. The filters were subsequently allowed to air dry for 30 minutes at room temperature. All probe solutions underwent three contact angle assessments on the substratum surface and bacterial lawns. Based on the MIC outcomes, the effect of TA and GA on PLA surface physicochemical properties was realised as follows: 0.0625 mg and 0.25 mg studied and diluted in dimethylsulfoxide (DMSO 2%) at the concentration of 0.0625 mg/mL and 0.25 mg/mL (MICs for *S. aureus* and *P. aeruginosa*, respectively) was applied by depositing it onto the PLA surface for 3 hours at room temperature (25 °C). After drying and adsorption of the product, the samples were immediately prepared for contact angle measurement.

Table 1: Energy characteristics (mJ.m⁻²) of pure liquid used to measure contact angles

Liquid	γ^{LW}	γ^+	γ^-
Water (w)	21.8	25.5	25.5
Formamide (F)	39.0	2.3	39.6
Diiomethane (D)	50.5	0	0

(γ^{LW}) Lifshitz-Van Der Waals of the surface free energy, (γ^+) electron donor, (γ^-) electron acceptor.

Hydrophobicity and surface free energy calculations

A 2 μ L drop of the test liquid was placed on the surface of the filter containing bacteria. Contact angles were measured 15 seconds after the drop had stabilized. For PLA contact angle measurements, the same procedure was used. The physicochemical parameters of sample surfaces derived using Young-Van Oss's equation (1) include the electron donor (γ^-), electron acceptor (γ^+), surface free energy (ΔG_{iwi}), and Lifshitz-Van Der Waals component (γ^{LW}).²⁹

$$(1 + \cos \theta) \gamma_L = 2 [(\gamma_S^{LW} \gamma_L^{LW})^{1/2}] + 2 [(\gamma_S^+ \gamma_L^-)^{1/2}] + 2 [(\gamma_S^- \gamma_L^+)^{1/2}] \quad (1)$$

With (θ) contact angle, (S) Solid surface, and (L) Liquid phase.

Wherein $\gamma_S^{AB} = 2(\gamma_S^- \gamma_S^+)^{1/2}$ is the component of acid-base free energy, and the surface free energy is shown as (2):

$$\gamma_s = \gamma_s^{LW} + \gamma_s^{AB} \quad (2)$$

The hydrophobicity of PLA and bacteria cell surfaces was assessed using contact angle measurements and the Van Oss method.³⁰ In this method, the free energy of interaction (ΔG_{iwi}) between two entities of a particular material (l) while submerged in water (w) is used to indicate how hydrophobic a substance is. The substance is referred to as hydrophobic ($\Delta G_{iwi} < 0$) or hydrophilic ($\Delta G_{iwi} > 0$) if the contact between the two entities is stronger than the interaction of each entity with water. The following formula is used to determine ΔG_{iwi} using the surface tension elements of the interacting entities (3):

$$\Delta G_{iwi} = -2\gamma_{iw} = -2 \left[((\gamma_i^{LW})^{1/2} - (\gamma_w^{LW})^{1/2})^2 + 2((\gamma_i^+ \gamma_i^-)^{1/2} (\gamma_w^+ \gamma_w^-)^{1/2} (\gamma_i^+ \gamma_w^-)^{1/2} (\gamma_w^+ \gamma_i^-)^{1/2}) \right] \quad (3)$$

With (γ^{LW}) Lifshitz-Van Der Waals component of the surface free energy, (γ^+) electron donor, (γ^-) electron acceptor.

Calculation of total free energy of interaction

The total interaction energy between bacteria (B) and a substrate (S) through water (W) (separated by a distance d) is determined by the sum of the Lifshitz-Van der Waals (G^{LW}), electrostatic double layer (G^{EL}), and acid-base interaction energies (G^{AB}).

The total contact or adhesion energy between a bacterium (spherical) and a substrate (flat plane) surface, is given as a consequence of the spacing (d), it can be calculated from the following way (4):

$$G^{DLVO}(d) = G^{LW}(d) + G^{EL}(d) \quad (4)$$

The acid-base energy (G^{AB}) should be taken into account in addition to the LW and EL interaction energies, in accordance with Van Oss *et al.*³¹ the total interaction energy (G^{XDLVO}) may be expressed as follows (5):

$$\Delta G^{XDLVO}(d) = \Delta G^{LW}(d) + \Delta G^{EL}(d) + \Delta G^{AB}(d) \quad (5)$$

With (6):

$$\Delta G_{MSL}^{LW} = ((\gamma_M^{LW})^{1/2} - (\gamma_S^{LW})^{1/2})^2 - ((\gamma_M^{LW})^{1/2} - (\gamma_L^{LW})^{1/2})^2 - ((\gamma_S^{LW})^{1/2} - (\gamma_L^{LW})^{1/2})^2 \quad (6)$$

And (7):

$$\Delta G^{AB} = 2[(\gamma_L^+)^{1/2} ((\gamma_M^-)^{1/2} + (\gamma_S^-)^{1/2} - (\gamma_L^-)^{1/2}) + (\gamma_L^-)^{1/2} ((\gamma_M^+)^{1/2} + (\gamma_S^+)^{1/2} - (\gamma_L^+)^{1/2}) - (\gamma_L^- \gamma_S^+)^{1/2} - (\gamma_L^+ \gamma_S^-)^{1/2}] p_{oo} \quad (7)$$

The electrical connections GEL were overlooked in the adhesion mechanism since the suspending solution (KNO_3) used in this experiment had a high ionic strength (0.1 M).³² Bacteria adhesion is favorable if $\Delta G^{XDLVO} < 0$ and unfavorable if $\Delta G^{XDLVO} > 0$.

Experimental adhesion essay

S. aureus and *P. aeruginosa* were grown on solid Luria Bertani (LB) substrate after being sub-cultured from glycerol. After 24 hours, the strains were inoculated in liquid Luria-Bertani medium (5 g yeast extract, 10 g peptone, 10 g NaCl, and 20 g Agar-agar per 1 litre of sterilised distilled water), then incubated at 37°C for 24 hours with stirring. Centrifugation at 5000 rpm for 15 minutes was used to collect bacterial cells. This step is crucial to concentrate the bacterial cells and remove any residual growth medium, ensuring that subsequent experiments are conducted with a consistent and defined bacterial suspension. The bacterial cells were rinsed twice with KNO_3 (0.1M), and vortexed with KNO_3 to create a bacterial suspension with an optical density of 0.4 to 0.5 at 600 nm (10^6 UFC/mL). This helps to ensure that the results are due to the interactions between the bacteria and the PLA surface rather than any residual media components. Following surface modification of the PLA materials with the investigated secondary metabolite, the adhesion of strains was done by sedimentation at 25 °C for 10 hours. The interfaces were dipped in 15 mL of the strain solution (10^6 cells/mL) and then retrieved and cells were washed with sterile distilled water to eliminate the bacteria that had not attached to the surface after the contact duration.³³ A scanning electron microscope (SEM) was used to examine the materials.

Scanning Electronic Microscopy (SEM)

For the adhesion verification process, the treated and untreated PLA tests were performed utilising a scanning electron microscope (JEOL, IT500 HR, Japan). To calculate the percentage of PLA surface occupied by bacteria strains, the SEM images were analysed using MATLAB software. MATLAB calculates adhesion by analysing the proportion of the total surface of 3D-printed PLA to the portion covered by bacterial cells.

Statistical analysis

Results were reported as the mean \pm standard deviation (mean \pm SD). All data were subjected to Tukey pairwise comparisons test, using the software package Minitab 19 with a level of significance of 5%. Correlational analysis was done using the Pearson test using the software package XLSTAT 2022.

Results and Discussion

Numerous researches have examined how bacteria interact with surfaces of varying roughness. According to previous works,^{27,34,35} the bacterial adhesion or anti-adhesion abilities varied depending on the surface roughness at the nanoscale and microscale levels. The surface roughness Ra reported in this investigation had a value of 0.45 ± 0.05 μ m and was centred in the submicron and micron region (0.1 to 10 μ m). Several data points have shown that bacterial adhesion to materials with submicron-range roughness increased as the roughness progressed until it reached the critical threshold.³⁶⁻³⁹ However, Almaguer-Flores *et al.* noted that the chemical properties of the surface played a crucial role in the colonial expansion of *E. corrodens* despite variations in surface roughness (0.028-1.83 μ m) or the culture medium employed.⁴⁰ The link between bacterial adhesion and surface roughness remains debatable, especially at the nanoscale. In fact, it was discovered that *S. aureus* cells may adhere to surfaces with an average roughness (Ra) smaller than 0.5 nm without restriction. *P. aeruginosa* cells, on the other hand, were discovered to be unable to colonise surfaces with an average roughness below 1 nm.⁴¹ Also, Yoda *et al.* mentioned that even a surface roughness of less than 30 nm Ra, might enhance bacterial adhesion.⁴² The previously mentioned findings suggest that the roughness level affecting bacterial adherence varies depending on the substance utilised and the microorganism's capacity to attach to different surfaces. The precise adhesion process is yet unknown due to a complicated interaction of various additional parameters relating to the bacterium itself, the *in vivo* environment, and the specific manufactured material used.^{32,43}

Similarly, the MIC was obtained using the microdilution technique and the colour marker resazurin. The MIC wells were those in which the resazurin colour stayed intact. As a result, the MIC values of TA against *P. aeruginosa* and *S. aureus* were MIC_{TAP}=0.25 mg/mL and MIC_{TAS}=0.625 mg/mL, respectively, whereas the MIC values of GA were MIC_{GAP}=0.039 mg/mL and MIC_{GAS}=0.156 mg/mL. Mandal *et al.* established that tannic acid has the greatest β -lactamase inhibition potential, primarily through *in vitro* screenings, and found it to be the most influential source with antibacterial properties, as well as abilities to suppress β -lactamase and biofilms against *P. aeruginosa*.⁴⁴ Equally, gallic acid showed a potential inhibitory effect against tetR and tetM of *Streptococci* spp., indicating that gallic acid is a remarkable therapeutic option to counteract tet-pump mediated tetracycline tolerance, pending further *in-vivo* confirmation.⁴⁵ The findings indicate that various bacterial species respond differently to the tested phenolic compounds.⁴⁶⁻⁴⁸ Broadly, Gram-negative bacteria, such as *P. aeruginosa*, tend to be more susceptible to these compounds in contrast to Gram-positive bacteria.⁴⁸ Specifically, Gallic acid exhibited limited effectiveness against *Bacillus subtilis* but showed sensitivity against *E. coli* and *P. aeruginosa*. Similarly, Tannic acid displayed moderate antibacterial activity against *Bacillus subtilis* and robust antimicrobial effects against *E. coli* and *P. aeruginosa*.^{47,48} Additionally, Payne *et al.* discovered that tannic acid effectively prevents the formation of *S.*

aureus biofilms without harming *S. aureus* bacterial growth.⁴⁹ This supports the theory that its biofilm inhibition is related to the IsaA transglycosylase mechanism.⁴⁹ A docking study has demonstrated before that tannic acid binds more strongly to *P. aeruginosa* target proteins, and it may be assumed that the phytochemical is more efficient against this pathogen. As a result, it can be employed as an effective antibacterial agent against *P. aeruginosa* Quorum sensing.⁵⁰

Furthermore, the contact angle measurements and calculations using the Young–Van Oss technique were used to estimate the surface physicochemical characteristics of untreated, treated PLA and *P. aeruginosa*, *S. aureus* strains, including hydrophobicity, acid-base parameters, and surface free energy (Table 2). The water contact angles (θ_w), which may be used to determine the surface hydrophobicity of a substance, are listed in Table 3. Typically, if θ_w is more than 90° and $\Delta G_{iwi} = 0$, the interface is hydrophobic, but if θ_w is less than 90° and $\Delta G_{iwi} > 0$, the surface is hydrophilic.⁵¹ As can be shown, the untreated PLA surface was hydrophilic qualitatively and hydrophobic quantitatively, with values of $\theta_w = 62.13 \pm 0.12^\circ$ and $\Delta G_{iwi} = -27.40 \text{ mJ.m}^{-2}$. The findings further revealed that the electron donor characteristic (γ^-) is more pronounced than the electron acceptor characteristic (γ^+) in PLA, with $\gamma^- = 14.66 \pm 0.19 \text{ mJ.m}^{-2}$ and $\gamma^+ = 0.64 \pm 0.05 \text{ mJ.m}^{-2}$, respectively. It also has a smaller acid-base component ($\gamma^{AB} = 10.38 \text{ mJ.m}^{-2}$) than the Lifshitz Van Der Waals parameter ($\gamma^{LW} = 42.03 \pm 0.09 \text{ mJ.m}^{-2}$). These align with those reported by other researchers,⁵² who found that the identical substance is hydrophilic ($\theta_w = 67.27^\circ$ and $\theta_w = 78^\circ$, respectively) and has poor acid-base characteristics. Furthermore, Badica *et al.*⁵³ discovered that this substratum has a relative hydrophobicity of $\theta_w = 95 \pm 1$. Moreover, Raouan *et al.*⁵⁴ revealed that the same bacterial surfaces exhibited strong hydrophilicity and a tendency to donate electrons while weakly accepting them. In addition, the surface of PLA displayed hydrophobic properties and a preference for electron donation. The findings demonstrated that both *P. aeruginosa* and *S. aureus* strains are qualitatively and quantitatively hydrophilic, with water contact angles of $\theta_w = 0.00 \pm 0.00^\circ$, $\theta_w = 9.77 \pm 0.35^\circ$ and $\Delta G_{iwi} = 30.24 \text{ mJ.m}^{-2}$ and $\Delta G_{iwi} = 29.60 \text{ mJ.m}^{-2}$, respectively. The findings also revealed that the strain under investigation is primarily an electron donor, with high values of $\gamma^- = 54.93 \pm 0.01 \text{ mJ.m}^{-2}$, $\gamma^- = 55.67 \pm 0.33 \text{ mJ.m}^{-2}$, and has a minor electron acceptor character, with $\gamma^+ = 1.94 \pm 0.01 \text{ mJ.m}^{-2}$, $\gamma^+ = 3.41 \pm 0.16 \text{ mJ.m}^{-2}$, respectively. It should be highlighted that both *P. aeruginosa* and *S. aureus* strains had a greater γ^{LW} value ($\gamma^{LW} = 37.54 \pm 0.06 \text{ mJ.m}^{-2}$ and $\gamma^{LW} = 29.86 \pm 0.37 \text{ mJ.m}^{-2}$, respectively) than γ^{AB} component ($\gamma^{AB} = -17.27 \text{ mJ.m}^{-2}$ and $\gamma^{AB} = -15.45 \text{ mJ.m}^{-2}$, respectively). In general, the hydrophilic property of a substance is significantly connected to its protein/carbohydrate ratio.³³ As a result, it is clear that the *P. aeruginosa* and *S. aureus* strains' hydrophilic characteristics tended to develop a greater protein/carbohydrate percentage. The bacteria surface cells also showed a preponderance of the electron donor factor, which matches the findings of van der *et al.*^{55,56} In addition, the quantity of acid-base groups and their characterisation have primarily been used to describe cell surface charge creation and substratum-bacterial interactions.⁵⁷⁻⁵⁹ In fact, amine groups have a negative

correlation with electron acceptor (acid) properties, while phosphate groups increase electron donor (base) properties. Higher polysaccharide levels and low protein quantities are also associated with the electron acceptor feature.⁶⁰ Surface properties of PLA play a crucial role in bacterial adhesion. The hydrophobicity of the surface, along with its acid-base parameters and surface free energy, significantly influences how bacteria adhere to it. Increased hydrophobicity and favourable acid-base interactions can enhance bacterial adhesion, whereas higher surface free energy typically leads to reduced adhesion. These findings are essential for understanding how modifications to the PLA surface can be used to control bacterial attachment, thereby meeting the broader research objectives of improving the antimicrobial properties of 3D-printed materials for medical applications.⁶¹

Data in Table 4 shows the influence of GA and TA (secondary metabolites) on surface free energy parameters. The treatment of the PLA surface with $\text{MIC}_{\text{TA/P}}$ and $\text{MIC}_{\text{GA/P}}$ changed and enhanced its hydrophilic nature. Indeed, the untreated PLA surface, which was hydrophilic qualitatively but hydrophobic quantitatively, became more hydrophilic qualitatively with contact angle values ranging from $\theta_w = 62.13 \pm 0.12^\circ$ to $9.03 \pm 0.06^\circ$ and $15.80 \pm 0.00^\circ$, respectively. Additionally, the surface's character transformed from hydrophobic ($\Delta G_{iwi} = -27.40 \text{ mJ.m}^{-2}$) to hydrophilic character with $\Delta G_{iwi}\text{-MIC}_{\text{TA/P}} = 30.72 \text{ mJ.m}^{-2}$ and $\Delta G_{iwi}\text{-MIC}_{\text{GA/P}} = 22.49 \text{ mJ.m}^{-2}$. Similarly, treating the PLA surface with $\text{MIC}_{\text{TA/S}}$ improved its hydrophilic character qualitatively, with contact angle data ranging from $\theta_w = 62.13 \pm 0.12^\circ$ to $0.00 \pm 0.00^\circ$. However, $\text{MIC}_{\text{GA/S}}$ treatment of the PLA surface increased its hydrophobic character from $\Delta G_{iwi} = -27.40 \text{ mJ.m}^{-2}$ to $-107.24 \text{ mJ.m}^{-2}$ without a notable change of θ_w . These data are compatible with those observed in prior studies.^{62,63} The findings showed that as the acrylic acid treatment increased, the contact angle dropped, indicating that PLA became more hydrophilic and exhibited antimicrobial capabilities, resulting in lower contact angle values from $\theta_w = 94.5^\circ$ to $\theta_w = 64.1^\circ$. Moreover, another study showed a decrease in contact angle value after ascorbic acid treatment from $\theta_w = 102.7 \pm 7.9^\circ$ to $\theta_w = 27.5 \pm 0.3^\circ$. Wenzel's wetting theory helps explain the reduction in contact angles following treatment.⁶⁴ Nevertheless, our results contradict those obtained by treating PLA surfaces with Halloysite Nanotubes (HNTs), which show that PLA/HNTs films become more hydrophobic.⁶⁵ In addition to hydrophobicity, the findings showed that after treatment, PLA's electron donor property increased. Thus, PLA surfaces processed with $\text{MIC}_{\text{TA/S}}$, $\text{MIC}_{\text{TA/P}}$, and $\text{MIC}_{\text{GA/P}}$ compounds became more electron-donating, with greater scores of $56.05 \pm 0.01 \text{ mJ.m}^{-2}$, $54.18 \pm 0.02 \text{ mJ.m}^{-2}$, and $49.87 \pm 0.03 \text{ mJ.m}^{-2}$ respectively, compared to PLA materials treated with $\text{MIC}_{\text{GA/S}}$ ($\gamma^- = 6.65 \pm 0.59 \text{ mJ.m}^{-2}$) and untreated PLA. In terms of the electron acceptor parameter, it was discovered that it increased slightly for GA and decreased slightly for TA. Similar findings were observed in the work of Badica *et al.*⁵³ which reported that after Mg treatment of PLA, the Lewis base (γ^-) characteristic increased. By contrast to the untreated PLA ($\gamma^- = 1.9 \pm 0.6 \text{ mJ/m}^2$ and $\gamma^+ = 0.6 \pm 0.3 \text{ mJ/m}^2$), electron donor components were found to vary from 1.9 ± 0.6 to $17.0 \pm 1.4 \text{ mJ/m}^2$, with constant electron acceptor values ($\gamma^+ = 0.6 \pm 0.1 \text{ mJ/m}^2$).

Table 2: Contact angle values, surface energies, and their components of PLA, *P. aeruginosa*, and *S. aureus*

Substrate	Contact angle ($^\circ$)			Surface energy: components and parameters (mJ.m^{-2})					
	θ_w	θ_F	θ_D	γ^{LW}	γ^+	γ^-	γ^{AB}	γ^{Tot}	ΔG_{iwi}
PLA	62.13 ± 0.12	40.27 ± 0.38	34.80 ± 0.20	42.03 ± 0.09	0.64 ± 0.05	14.66 ± 0.19	10.38	52.41	-27.40
<i>P. aeruginosa</i>	0.00 ± 0.00	0.00 ± 0.00	43.87 ± 0.12	37.54 ± 0.06	1.94 ± 0.01	54.93 ± 0.01	-17.27	20.27	30.24
<i>S. aureus</i>	9.77 ± 0.35	16.43 ± 0.50	57.67 ± 0.65	29.86 ± 0.37	3.41 ± 0.16	55.67 ± 0.33	-15.45	14.41	29.60

(θ_w) Contact angle, (γ^{LW}) Lifshitz-Van Der Waals of the surface free energy, (γ^+) electron donor, (γ^-) electron acceptor, (ΔG_{iwi}) the surface free energy and (γ^{AB}) The acid-base surface tension component.

Table 3: Contact angle values, surface energies, and their components of untreated PLA (witness), Treated PLA with TA and GA, and *S. aureus*.

Substrate	Contact angle (°)			Surface (mJ.m ⁻²)	Energy: components and parameters				
	θ_w	θ_F	θ_D		γ^{LW}	γ^+	γ^-	γ^{AB}	γ^{Tot}
Untreated PLA	62.13 ± 0.12	40.27 ± 0.38	34.80 ± 0.20	42.03 ± 0.09	0.64 ± 0.05	14.66 ± 0.19	10.38	52.41	-27.40
Treated PLA-MIC _{TA/S}	0.00 ± 0.00	0.00 ± 0.00	17.20 ± 0.35	48.45 ± 0.09	0.30 ± 0.01	56.05 ± 0.01	15.39	63.84	-41.26
Treated PLA- MIC _{GA/S}	64.83 ± 0.74	25.73 ± 0.06	40.20 ± 0.00	39.43 ± 0.00	3.75 ± 0.11	6.65 ± 0.59	51.00	90.43	-107.24
Treated PLA-MIC _{TA/P}	9.03 ± 0.06	0.00 ± 0.00	21.67 ± 0.38	47.18 ± 0.12	0.45 ± 0.01	54.18 ± 0.02	-20.24	26.94	30.72
Treated PLA- MIC _{GA/P}	15.80 ± 0.00	8.80 ± 0.10	58.27 ± 0.15	29.51 ± 0.09	4.44 ± 0.04	49.87 ± 0.03	-11.84	17.67	22.49

Table 4: Pearson correlation matrix between physicochemical parameters (θ_w , γ^+ , γ^- , γ^{LW} and ΔG_{iwi})

Variables	θ_w			γ^+			γ^-			γ^{LW}			ΔG_{iwi}		
	r	p-value	r ²	r	p-value	r ²	r	p-value	r ²	r	p-value	r ²	r	p-value	r ²
θ_w	1	0	1	0.592	0.020	0.350	-0.984	0.000	0.968	-0.577	0.024	0.333	-0.627	0.012	0.394
γ^+	0.592	0.020	0.350	1	0	1	-0.562	0.029	0.316	-0.797	0.000	0.636	-0.213	0.446	0.045
γ^-	-0.984	<0,0001	0.968	-0.562	0.029	0.316	1	0	1	0.458	0.086	0.210	0.747	0.001	0.558
γ^{LW}	-0.577	0.024	0.333	-0.797	0.000	0.636	0.458	0.086	0.210	1	0	1	-0.067	0.812	0.005
ΔG_{iwi}	-0.627	0.012	0.394	-0.213	0.446	0.045	0.747	0.001	0.558	-0.067	0.812	0.005	1	0	1

Values in bold are different from 0 with a significance level alpha = 0,05

Table 5: Tukey pairwise comparisons of mean treatments

Treatments	Grouping Information Using the Tukey Method and 95% Confidence											
	θ_w			γ^+			γ^-			γ^{LW}		
	N	Mean	Grouping	N	Mean	Grouping	N	Mean	Grouping	N	Mean	Grouping
Untreated PLA	3	62,1333	b	3	2,9176	c	3	18,5455	d	3	26,125	e
Treated PLA- MIC _{GA/S}	3	64,833	a	3	3,7533	b	3	6,647	e	3	39,43	c
Treated PLA- MIC _{GA/P}	3	15,80	c	3	4,4433	a	3	49,8733	c	3	29,5100	d
Treated PLA-MIC _{TA/P}	3	9,0333	d	3	0,44667	d	3	54,1800	b	3	47,1767	b
Treated PLA-MIC _{TA/S}	3	0,000000	e	3	0,30333	d	3	56,0467	a	3	48,4500	a

Means that do not share a letter are significantly different.

To our knowledge, the relationship between physicochemical parameters (θ_w , γ^+ , γ^- , γ^{LW} , and ΔG_{iwi}) on PLA modified with natural products has not been previously studied. Therefore, a Pearson correlation test was performed between each physicochemical parameter and another based on untreated and treated PLA data to measure the strength and direction of linear correlation (Table 5). The results showed a very strong correlation between θ_w and γ^- with a correlation coefficient value of -0.984 and a p-value < 0.0001 (Table 5, Figure 1 a). Additionally, the coefficient of determination (r^2) for the same correlation was 0.968, indicating that 96.8% of the variability in θ_w is explained by the variability in γ^- and vice versa. Furthermore, the test displayed a strong correlation firstly between γ^+ and γ^{LW} , and secondly between γ^- and ΔG_{iwi} with a correlation coefficient value of -0.797 and 0.747, respectively (Table 5, Figure 1 b and c). However, a moderate correlation was found between θ_w and ΔG_{iwi} ($r = -0.627$). Aside from hydrophobicity and electron donor and acceptor characteristics, the total surface free energy of PLA was also marginally affected by treatment. Specifically, the treatments yielded greater values of $\gamma^{Tot} = 63.84 \text{ mJ.m}^{-2}$ and $\gamma^{Tot} = 90.43 \text{ mJ.m}^{-2}$ for PLA-MIC_{TA/S} and PLA-MIC_{GA/S}, respectively. However, the samples treated with PLA-MIC_{TA/P} and PLA-MIC_{GA/P} fractions yielded lower values of 26.94 mJ.m^{-2} and 17.67 mJ.m^{-2} , respectively, compared to the untreated PLA. Similar findings to the PLA-MIC_{TA/S} and PLA-MIC_{GA/S} treatments were reported in the study of Luque-Agudo *et al.*⁶⁶ which demonstrated that following Mg processing of PLA, the total surface free energy (γ^{Tot}) property increased. Specifically, their research indicated that the total surface free energy of PLA was observed to range from 25 ± 2 to $30 \pm 3 \text{ mJ/m}^2$ when compared to untreated PLA, which had a total surface free energy of $25 \pm 2 \text{ mJ/m}^2$. Moreover, the Tukey pairwise comparisons test of physicochemical parameters (θ_w , γ^+ , γ^- and γ^{LW}) between untreated PLA and all treatments performed are presented in Table 6. The Tukey method of grouping information revealed that the means of θ_w , γ^+ , γ^- and γ^{LW} of all the treatments (of TA and GA chemicals) on PLA varied significantly from the θ_w , γ^+ , γ^- and γ^{LW} of the untreated PLA (i.e., the untreated PLA means of θ_w , γ^+ , γ^- and γ^{LW} do not share the same letter of all treatments performed which indicates that the means are significantly different). In this manner, the treatments with TA and GA have a substantial impact on the physicochemical properties of PLA surfaces, including hydrophobicity, donor/acceptor electron characters, and surface-free energy. Tannic acid is a phenolic acid and natural tannin composed of a central glucose unit with ten gallic acid molecules bonded to it, indicating that the two molecules (TA and GA) share the same chemical groups.¹⁰ The numerous hydroxyl groups in

TA (twenty-five hydroxyl groups) and GA (three hydroxyl groups) interface with molecules and biomaterials including proteins, digestive enzymes, carbohydrates, and minerals, endowing TA and GA-based compositions with a variety of fascinating physical and chemical characteristics.^{67,68} Additionally, hydroxybenzoic acids (such as GA) with a minor degree of hydroxylation in phenol groups, strongly methoxylated phenol groups, or ester derivatives with long alkyl chains exhibit stronger antibacterial activity compared to their parent structures.⁶⁹

In the bacterial adhesion process, both the physicochemical characteristics of the bacterial cell and the material interface play pivotal roles. Understanding these processes is essential for regulating and preventing adhesion. Therefore, predicting the adherence of *S. aureus* and *P. aeruginosa* to untreated and treated PLA substrates is crucial. This involves using various MICs of TA and GA chemicals and identifying the factors that influence adhesion on these PLA materials. Consequently, estimates of the total interaction-free energy in the adhesion process on both unmodified and modified PLA were made. It's important to note that in this study, the suspending solution (KNO₃) had a significant ionic strength, so the electrical interactions (ΔG^{EL}) were not considered in the adhesion mechanism.⁷⁰ Table 7 shows the free energy of interaction between *S. aureus*, *P. aeruginosa*, and PLA surfaces. According to these findings, the total free energies of untreated PLA and both strains are positive ($\Delta G^{XDLVO} = 9.80 \text{ mJ.m}^{-2} > 0$ for *S. aureus* and $\Delta G^{XDLVO} = 5.85 \text{ mJ.m}^{-2} > 0$ for *P. aeruginosa*), suggesting that adhesion is unfavourable. Likewise, the ΔG^{XDLVO} values of *S. aureus* and *P. aeruginosa* rose following PLA surface treatment. Furthermore, the findings revealed that the PLA-MIC_{TA/S} treatment ($\Delta G^{XDLVO} = 33.60 \text{ mJ.m}^{-2}$) yielded the greatest value of ΔG^{XDLVO} , followed by PLA-MIC_{TA/P} and PLA-MIC_{GA/P} treatments with total free energy interactions of 31.08 mJ.m^{-2} and 26.34 mJ.m^{-2} , respectively. However, following PLA treatment with MIC_{GA/S}, the ΔG^{XDLVO} value decreased ($\Delta G^{XDLVO} = -3.35 \text{ mJ.m}^{-2}$), indicating that adhesion is beneficial for the treated PLA- MIC_{GA/S}. Furthermore, it was observed that the negative value of the ΔG^{AB} parameter was larger than the ΔG^{LW} component in the situation of treated PLA- MIC_{GA/S} ($\Delta G^{XDLVO} < 0$) (Table 7). This indicates that medium to long-range forces, specifically acid-base interactions, may significantly influence the potential adhesion of *S. aureus* to treated PLA- MIC_{GA/S} material. Moreover, on all treatments, the ΔG^{LW} component was found to be negative, suggesting that all wide-ranging (Van Der Waals interactions) and relatively short-distance would lead to *S. aureus* and *P. aeruginosa* PLA adhesion.

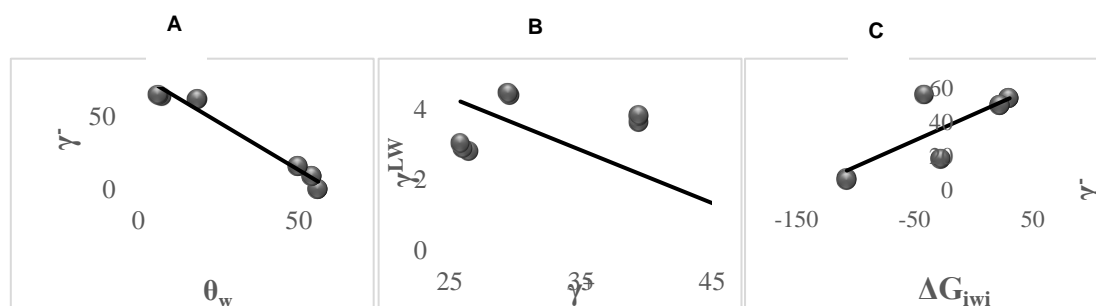


Figure 1: Pearson correlation between physicochemical parameters (θ_w , γ^+ , γ^- , γ^{LW} and ΔG_{iwi}). (A) Pearson correlation between θ_w and γ^- , (B) Pearson correlation between θ_w and γ^+ and γ^{LW} (C) Pearson correlation between ΔG_{iwi} and γ^- .

Table 6: ΔG^{XDLVO} (mJ.m^{-2}) interaction free energy

Substrata / Strain	ΔG^{LW}	ΔG^{AB}	ΔG^{XDLVO}
PLA / <i>S. aureus</i>	-2.99	12.80	9.80
Treated PLA-MIC _{TA/S}	-3.78	37.38	33.60
Treated PLA- MIC _{GA/S}	-2.66	-0.689	-3.35
PLA / <i>P. aeruginosa</i>	-5.43	11.28	5.85
Treated PLA-MIC _{TA/P}	-6.57	37.65	31.08
Treated PLA- MIC _{GA/P}	-2.32	28.66	26.34

The study also shows that *S. aureus* and *P. aeruginosa* can stick to the PLA material (Figure 2) with adhesion rates of 83.90% and 90.08%, respectively (Table 7). The SEM image analysis revealed that during treatment, the proportion of adhesion decreased. Similarly, *P. aeruginosa* was unable to attach to treated PLA-MIC_{GA/P} (Figure 4), but moderately adhered to treated PLA-MIC_{TA/P} (Figure 3) with a percentage of adhesion of 23.53%. *S. aureus*, on the other hand, only adhered weakly to treated PLA-MIC_{TA/S} and treated PLA-MIC_{GA/S}, with percentage adhesion of 8.43% and 4.27%, respectively (Figure 3 and Figure 4). It is widely recognised that the hydrophilic and hydrophobic properties of the material play a crucial influence on bacterial adherence. Olewnik-Kruszkowska *et al.* demonstrated that bacteria adhere more easily to hydrophobic surfaces than to hydrophilic ones.⁷¹ Furthermore, research has indicated that hydrophobic bacterial cells adhere more strongly to hydrophobic surfaces than hydrophilic cells adhere to hydrophilic surfaces.⁷² Our findings corroborate these assertions. Similarly, with modifications that made the surface more hydrophilic, the adherence of *S. aureus* and *P. aeruginosa* (hydrophilic) on PLA material was shown to diminish. Additionally, data demonstrated that superhydrophilic or superhydrophobic surfaces can be produced by manufactured materials and surface treatments, which can reduce bacterial adhesion.⁷³⁻⁷⁸ Furthermore, hydrophilic substrates have weaker adhesion than hydrophobic substrates, according to Verhorst *et al.* which is associated properly with our findings. Apart from hydrophobicity, by using the surface free energy factor to characterise the substrate, several scientists investigated the relationship

between bacterial adherence and material physical-chemical parameters. Tsibouklis *et al.*⁷⁹ found that low surface free energy polymer substrates inhibited bacterial attachment significantly, whereas some found that attachment was modest within certain surface free energy regions.⁸⁰ These assertions are consistent with our findings, especially with treatments PLA-MIC_{TA/S}, PLA-MIC_{GA/S}, and PLA-MIC_{GA/P} ($\Delta G_{\text{IWI}} = -41.26 \text{ mJ.m}^{-2}$, $\Delta G_{\text{IWI}} = -107.24 \text{ mJ.m}^{-2}$ and $\Delta G_{\text{IWI}} = 22.49 \text{ mJ.m}^{-2}$, respectively), which have shown notable *S. aureus* and *P. aeruginosa* adhesion inhibition. This study highlights the antiadhesive effects of tannic acid (TA) and gallic acid (GA) secondary metabolites on *S. aureus* and *P. aeruginosa*, which are linked to changes in the physicochemical properties of PLA. These changes make the PLA more hydrophilic and increase its electron donor characteristics while reducing electron acceptor traits. As a result, the interaction between bacteria and the material is weakened, leading to reduced bacterial adherence to PLA. This finding is particularly significant for medical and industrial applications, where decreased bacterial adhesion on treated PLA surfaces can enhance the performance and safety of medical devices and other PLA-based products. The study therefore provides valuable insights into how manipulating hydrophilicity, electron donor/acceptor characteristics, and surface free energy can achieve desired antimicrobial effects. By incorporating tannic acid and gallic acid into PLA surfaces, this research presents a promising approach to improving the material's antimicrobial properties, potentially leading to more reliable and effective applications in both medical and industrial contexts.

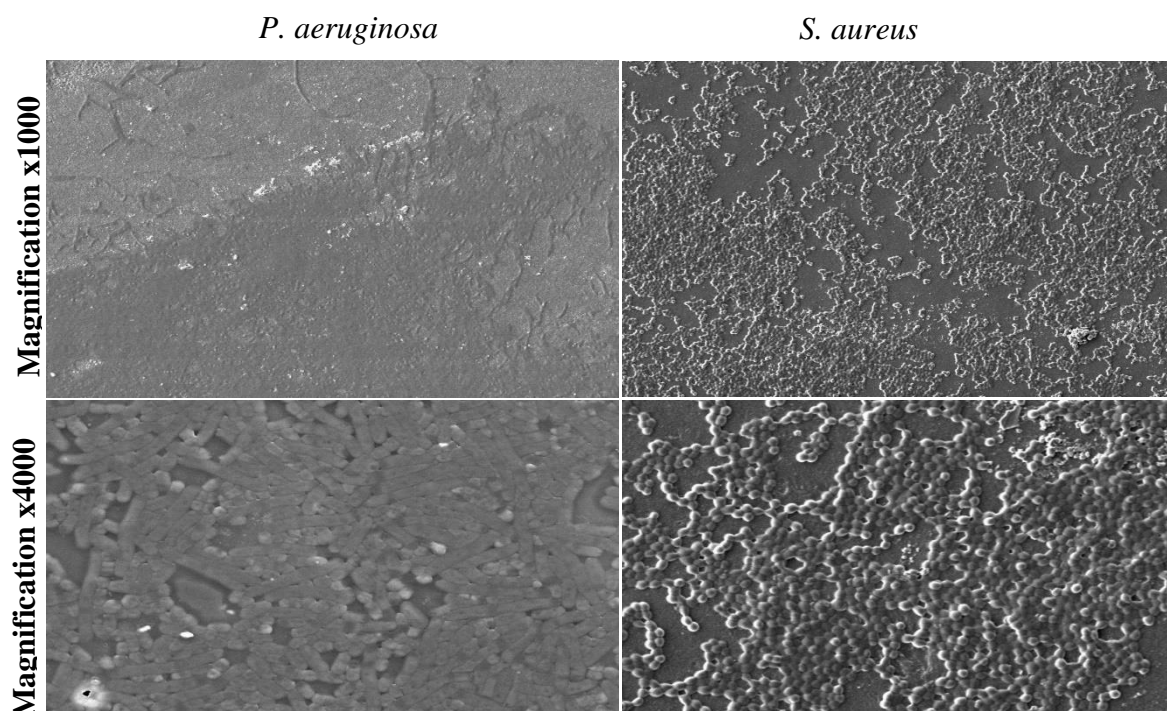


Figure 2: SEM observation of *S. aureus* and *P. aeruginosa* adhesion on untreated 3D printed PLA (before treatment).

Table 7: Percentage adhesion of *S. aureus* and *P. aeruginosa* bacteria on PLA before and after treatment

Bacterium	% Of Adhesion		
	Untreated PLA	Treated PLA by TA (% of inhibition)	Treated PLA by GA (% of inhibition)
<i>S. aureus</i>	83.90	9.43 (90.57%)	4.27 (95.73%)
<i>P. aeruginosa</i>	90.08	23.53 (76.47%)	0 (100%)

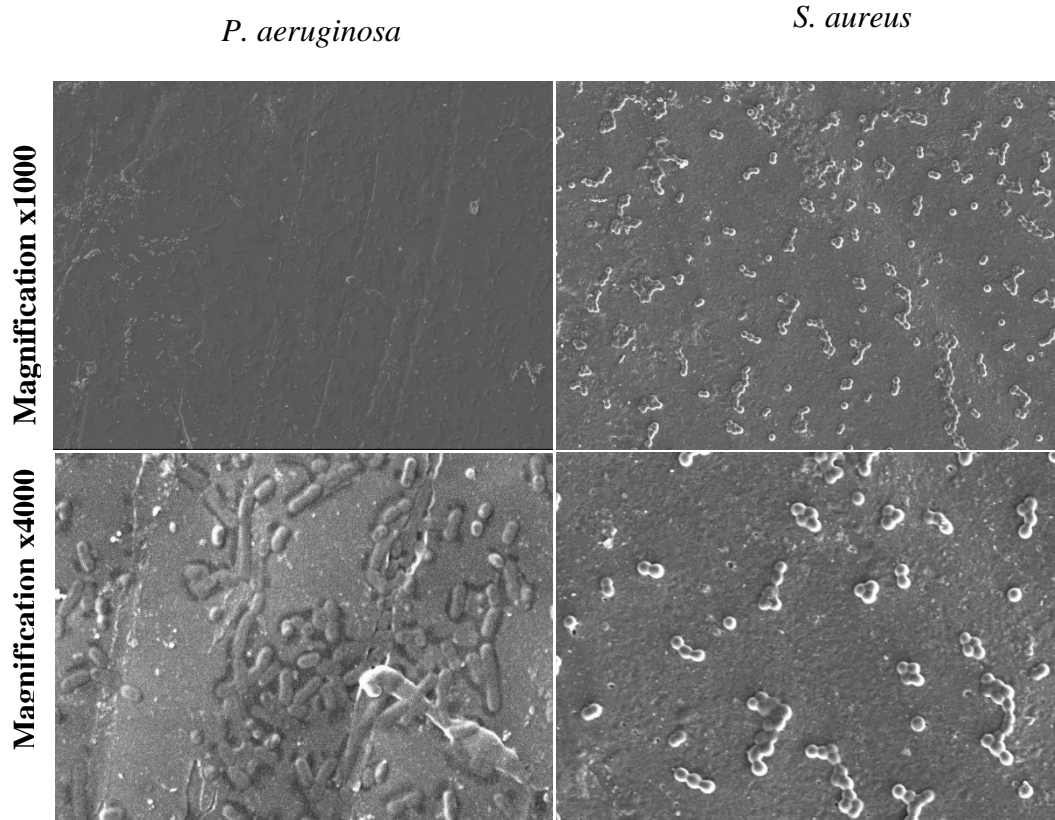


Figure 3: SEM observation of *S. aureus* and *P. aeruginosa* adhesion on treated 3D printed PLA with tannic acid

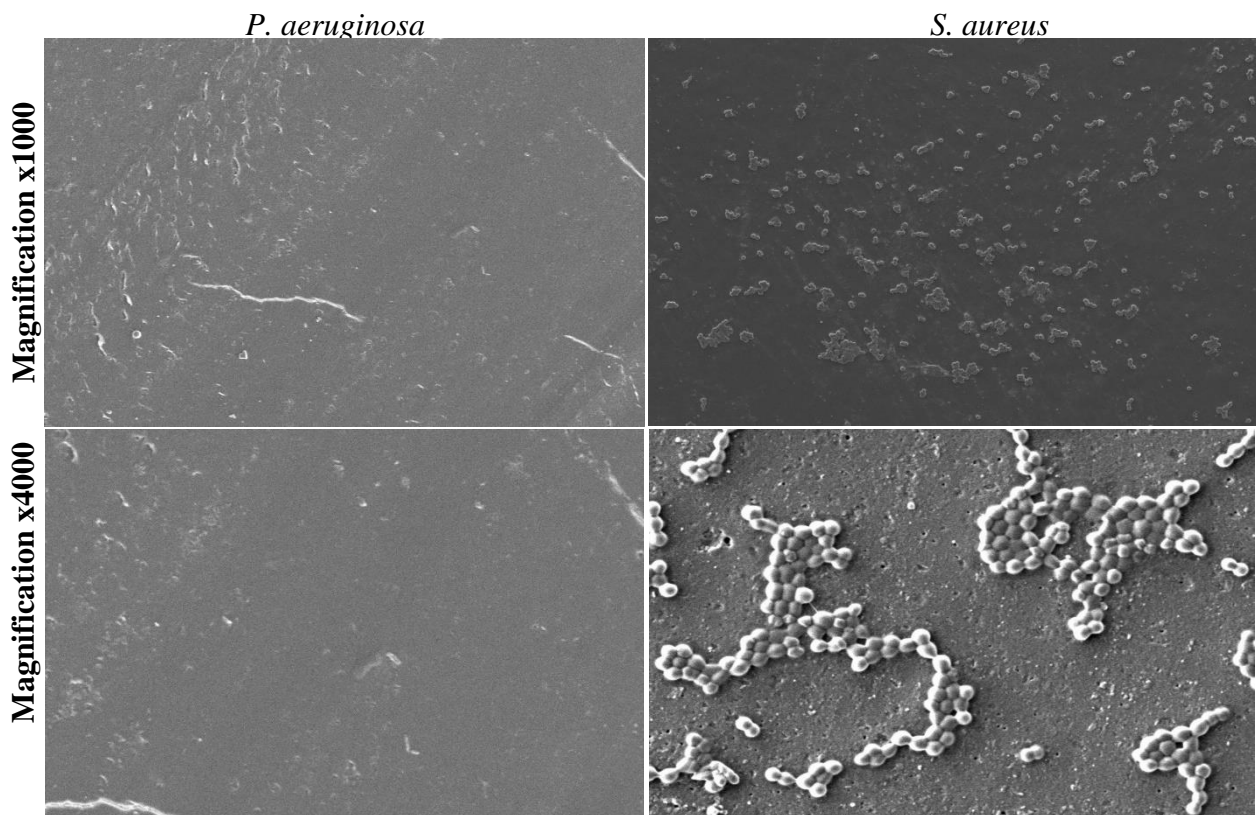


Figure 4: SEM observation of *S. aureus* and *P. aeruginosa* adhesion on treated 3D printed PLA with gallic acid.

Conclusion

This study evaluated the effects of gallic acid (GA) and tannic acid (TA) on 3D-printed polylactic acid (PLA), increasing its hydrophilicity and electron donor properties. Adhesion of *Pseudomonas aeruginosa* and *Staphylococcus aureus* was reduced, with MIC_{GAP} treatment achieving 100% inhibition. The results suggest PLA reinforced with plant metabolites as a promising antibacterial material for medical applications, with future research exploring encapsulation techniques to enhance these properties further.

Conflict of Interest

The authors declare no conflict of interest.

Authors' Declaration

The authors hereby declare that the work presented in this article is original and that any liability for claims relating to the content of this article will be borne by them.

Acknowledgments

We would like to thank the Moroccan Ministry of Higher Education, Scientific Research and Innovation and the OCP Foundation who funded this work through the APRD research program.

References

- Edwardson S, Cairns C. Nosocomial infections in the ICU. *J Anesth Analg Crit Care*. 2019; 20(1):14–18.
- Ma YX, Wang CY, Li YY, Li J, Wan QQ, Chen JH, Tay FR, Niu LN. Considerations and Caveats in Combating ESKAPE Pathogens against Nosocomial Infections. *Adv Sci*. 2020; 7(1):1901872.
- Roberto P, Moreno H, Inácio Da Costa-Issa F, Rajca-Ferreira AK, Pereira MAA, Kaneko TM. Native Brazilian Plants Against Nosocomial Infections: A Critical Review on their Potential and the Antimicrobial Methodology. *Curr Top Med Chem*. 2013; 13(24):3040–3078.
- Jamal M, Ahmad W, Andleeb S, Jalil F, Imran M, Nawaz MA, Hussain T, Ali M, Rafiq M, Kamil MA. Bacterial biofilm and associated infections. *J Chin Med Assoc*. 2018; 81(1):7–11.
- Utami DT, Hertiani T, Pratiwi SUT, Haniastuti T, Randy A, Priyanto JA, Prastya ME. Correlation Analyses of the Oral Biofilm Growth Inhibition Towards Hydrophobicity Reduction of Oral Pathogenic Bacteria. *Trop J Nat Prod Res*. 2023; 7(10):4141–4145.
- Zobell CE. The effect of solid surfaces upon bacterial activity. *J Bacteriol*. 1943; 46(1):39–56.
- Hermansson M. The DLVO theory in microbial adhesion. *Colloids Surf B Biointerfaces*. 1999; 14(1–4):105–119.
- Dong G, Liu H, Yu X, Zhang X, Lu H, Zhou T, Cao J. Antimicrobial and anti-biofilm activity of tannic acid against *Staphylococcus aureus*. *Nat Prod Res*. 2018; 32(18):2225–2228.
- Zarandona I, Puertas AI, Dueñas MT, Guerrero P, de la Caba K. Assessment of active chitosan films incorporated with gallic acid. *Food Hydrocoll*. 2020; 101:105486.
- Kaczmarek B. Tannic acid with antiviral and antibacterial activity as a promising component of biomaterials-A minireview. *Materials*. 2020; 13(14):3224.
- AL Zahrani NA, El-Shishtawy RM, Asiri AM. Recent developments of gallic acid derivatives and their hybrids in medicinal chemistry: A review. *Eur J Med Chem*. 2020; 204:112609.
- Alibi S, Crespo D, Navas J. Plant-derivatives small molecules with antibacterial activity. *Antibiotics*. 2021; 10(3):1–19.
- Kaczmarek B. Tannic acid with antiviral and antibacterial activity as a promising component of biomaterials-A minireview. *Materials*. 2020; 13(14):3224.
- Panthong S, Sakpakdeejaroen I, Kuropakornpong P, Jaicharoensub J, Itharat A. Antibacterial activity and stability evaluation of “Apo-taat” remedy extract for inhibiting diarrhoea-causing bacteria. *Trop J Nat Prod Res*. 2020; 4(12):1101–1107.
- Cheng YF, Pranantyo D, Kasi G, Lu ZS, Li CM, Xu LQ. Amino-containing tannic acid derivative-mediated universal coatings for multifunctional surface modification. *Biomater Sci*. 2020; 8(8):2120–2128.
- Badra B, Moustapha Soungalo D, Hafidha K, Rimmibtiri S, Muhammad AS, Aly S. Antimicrobial, Antibiofilm, And Biofilm Effects Of Gallic Acid On Exopolysaccharide-Dependent And -Independent Biofilm Of Model Strains *Streptococcus Thermophilus* Cnrz 447 And *Staphylococcus aureus* Atcc 43300. *J Microbiol Biotechnol Food Sci*. 2022; e1781.
- Lang S, Chen C, Xiang J, Liu Y, Li K, Hu Q, Liu G. Facile and Robust Antibacterial Functionalization of Medical Cotton Gauze with Gallic Acids to Accelerate Wound Healing. *Ind Eng Chem Res*. 2021; 60(28):10225–10234.
- Shahrubudin N, Lee TC, Ramlan R. An overview on 3D printing technology: Technological, materials, and applications. *Procedia Manuf*. 2019; 35:1286–1296.
- Bayraktar I, Doganay D, Coskun S, Kaynak C, Akca G, Unalan HE. 3D printed antibacterial silver nanowire/polylactide nanocomposites. *Compos B Eng*. 2019; 172:671–678.
- Rengier F, Mehndiratta A, Von Tengg-Kobligh H, Zechmann CM, Unterhinninghofen R, Kauczor HU, Giesel FL. 3D printing based on imaging data: Review of medical applications. *Int J Comput Assist Radiol Surg*. 2010; 5(4):335–341.
- Yan Q, Dong H, Su J, Han J, Song B, Wei Q, Shi Y. A Review of 3D Printing Technology for Medical Applications. *Eng*. 2018; 4(5):729–742.
- Hall DC, Palmer P, Ji HF, Ehrlich GD, Król JE. Bacterial Biofilm Growth on 3D-Printed Materials. *Front Microbiol*. 2021; 12:646303
- McGuffie BA, Vallet-Gely I, Dove SL. σ factor and anti- σ factor that controls swarming motility and biofilm formation in *Pseudomonas aeruginosa*. *J Bacteriol*. 2016; 198(5):755–765.
- Ford CA, Hurford IM, Cassat JE. Antivirulence Strategies for the Treatment of *Staphylococcus aureus* Infections: A Mini Review. *Front Microbiol*. 2021; 11:632706.
- CLSI. Methods for Dilution Antimicrobial Susceptibility Tests for Bacteria That Grow Aerobically. CLSI. 2012; 32(2):1–68.
- Zisman WA. Influence of Constitution on Adhesion. *Ind. Eng. Chem*. 1963; 55(10):18–38.
- Alhashmi Alamer F, Althagafy K, Alsalmi O, Aldeih A, Alotaiby H, Althebaiti M, Alghamdi H, Alotibi N, Saeedi A, Zabarmawi Y, Hawsawi M, Alnefaie MA. Review on PEDOT: PSS-Based Conductive Fabric. *ACS Omega*. 2022; 7(40):35371–35386.
- Sadiki M, Elabed S, Barkai H, Balouiri M, Nasri A, Koraichi SI. The modification of cedar wood surface properties for the prevention of fungal adhesion. *Int J Adhes Adhes*. 2017; 75:40–46.
- Van Oss CJ. The forces involved in bioadhesion to flat surfaces and particles – their determination and relative roles. *Biofouling*. 1991; 4(1–3):25–35.

30. Van Oss CJ. Development and applications of the interfacial tension between water and organic or biological surfaces. *Colloids Surf B Biointerfaces*. 2007; 54(1):2–9.
31. Van Oss CJ. Acid-base interfacial interactions in aqueous media. *Colloids Surf A Physicochem Eng Asp*. 1993; 78:1–49.
32. Zouine N, Raouan SE, Elharchli E, El Ghachtouli N, El Abed S, Sadiki M, IBN Souda Koraichi S. Theoretical and experimental investigations of *Staphylococcus aureus* and *Pseudomonas aeruginosa* adhesion on 3D printed resin. *Int J Adhes Adhes*. 2022; 118:103234.
33. Soumya E, Saad IK, Abdellah H, Hassan L. Experimental and theoretical investigations of the adhesion time of Penicillium spores to cedar wood surface. *Mater Sci Eng C*. 2013; 33(3):1276–1281.
34. Dufréne YF, Viljoen A, Mignolet J, Mathelié-Guinlet M. AFM in cellular and molecular microbiology. *Cell Microbiol*. 2021; 23(7):13324.
35. Kreve S, Reis ACD. Bacterial adhesion to biomaterials: What regulates this attachment? A review. *Jpn Dent Sci Rev*. 2021; 57:85–96.
36. Alam F, Balani K. Adhesion force of *Staphylococcus aureus* on various biomaterial surfaces. *J Mech Behav Biomed Mater*. 2017; 65:872–880.
37. Mei L, Busscher HJ, Van Der Mei HC, Ren Y. Influence of surface roughness on streptococcal adhesion forces to composite resins. *Dent Mater*. 2011; 27(8):770–778.
38. Wang C, Zhao Y, Zheng S, Xue J, Zhou J, Tang Y, Jiang L, Li W. Effect of enamel morphology on nanoscale adhesion forces of Streptococcal bacteria: An AFM study. *Scanning*. 2015; 37(5):313–321.
39. Yang K, Shi J, Wang L, Chen Y, Liang C, Yang L, Wang LN. Bacterial anti-adhesion surface design: Surface patterning, roughness, and wettability: A review. *J Mater Sci Technol*. 2022; 99:82–100.
40. Bui VD, Mwangi JW, Schubert A. Powder mixed electrical discharge machining for antibacterial coating on titanium implant surfaces. *J Manuf Process*. 2019; 44:261–270.
41. Truong VK, Pham VTH, Medvedev A, Lapovok R, Estrin Y, Lowe TC, Baulin V, Boshkovikj V, Fluke CJ, Crawford RJ, Ivanova EP. Self-organised nanoarchitecture of titanium surfaces influences the attachment of *Staphylococcus aureus* and *Pseudomonas aeruginosa* bacteria. *Appl Microbiol Biotechnol*. 2015; 99(16):6831–6840.
42. Oliveira WF, Silva PMS, Silva RCS, Silva GMM, Machado G, Coelho LCBB, Correia MTS. *J Hosp Infect*. 98(2):111–117.
43. Yoda I, Koseki H, Tomita M, Shida T, Horiuchi H, Sakoda H, Osaki M. Effect of surface roughness of biomaterials on *Staphylococcus epidermidis* adhesion. *BMC Microbiol*. 2014; 14(1):234.
44. Mandal SM, Dias RO, Franco OL. Phenolic Compounds in Antimicrobial Therapy. *J Med Food*. 2017; 20(10):1031–1038.
45. Sivakumar S, Smiline Girija AS, Vijayashree Priyadharsini J. Evaluation of the inhibitory effect of caffeic acid and gallic acid on tetR and tetM efflux pumps mediating tetracycline resistance in *Streptococcus sp.*, using computational approach. *J King Saud Univ Sci*. 2020; 32(1):904–909.
46. He W, Zhang Z, Chen J, Zheng Y, Xie Y, Liu W, Wu J, Mosselhy DA. Evaluation of the anti-biofilm activities of bacterial cellulose-Tannic acid-magnesium chloride composites using an in vitro multispecies biofilm model. *Regen Biomater*. 2021; 8(6):rbab054
47. Tintino SR, Morais-Tintino CD, Campina FF, Costa M do S, Menezes IRA, de Matos YMLS, Calixto-Júnior JT, Pereira PS, Siqueira-Junior JP, Leal-Balbino TC, Coutinho HDM, Balbino VQ. Tannic acid affects the phenotype of *Staphylococcus aureus* resistant to tetracycline and erythromycin by inhibition of efflux pumps. *Bioorg Chem*. 2017; 74:197–200.
48. Tyagi B, Dubey A, Kumar Verma B, Tiwari S. Antibacterial activity of phenolics compounds against pathogenic bacteria. *Int. J. Pharm. Sci. Rev. Res*. 35(1):16-18.
49. Payne DE, Martin NR, Parzych KR, Rickard AH, Underwood A, Boles BR. Tannic acid inhibits *Staphylococcus aureus* surface colonization in an isaA-dependent manner. *Infect Immun*. 2013; 81(2):496–504.
50. Bora N, Nath Jha A. Tannic acid: an efficient quorum sensing inhibitor. *Int Conf Syst Process Phys Chem Biol*. 2018; 1-4.
51. Baran EH, Yildirim Erbil H. Surface Modification of 3D Printed PLA Objects by Fused Deposition Modeling: A Review. *Colloids Interfaces* 2019; 3(2):43.
52. Li L, Ding S, Zhou C. Preparation and Degradation of PLA/Chitosan Composite Materials. *J Appl Polym Sci*. 2003; 91(1):274–277.
53. Badica P, Batalu ND, Balint E, Tudor N, Barbuceanu F, Peteoaca A, Micsa C, Eremia AD, Trancu OI, Burdusel M, Grigorescu MA, Aldica G V., Radu D, Porosnicu I, Tiseanu I. MgB₂-based biodegradable materials for orthopaedic implants. *J Mater Res Technol*. 2022; 20:1399–1413.
54. Raouan SE, Zouine N, Harchli E El, EL Abed S, Sadiki M, Ghachtouli N El, Lachkar M, Ibsouda SK. The theoretical adhesion of *Staphylococcus aureus* and *Pseudomonas aeruginosa* as nosocomial pathogens on 3D printing filament materials. *Folia Microbiol*. 2023; 68(4):627–632.
55. Van Der Mei HC, Bos R, Busscher HJ. A reference guide to microbial cell surface hydrophobicity based on contact angles. *Colloids Surf B Biointerfaces*. 1998; 11(4):213–221.
56. Shen L, Wang X, Li R, Yu H, Hong H, Lin H, Chen J, Liao BQ. Physicochemical correlations between membrane surface hydrophilicity and adhesive fouling in membrane bioreactors. *J Colloid Interface Sci*. 2017; 505:900–909.
57. Fern JB, Daughney CJ, Yee N, Davis TA. A chemical equilibrium model for metal adsorption onto bacterial surfaces. *Geochim Cosmochim Acta*. 1997; 61(16):3319–3328.
58. Yee N, Fein J. Cd adsorption onto bacterial surfaces: A universal adsorption edge? *Geochim Cosmochim Acta*. 2001; 65(13):2037–2042.
59. Hong Y, Brown DG. Cell surface acid-base properties of *Escherichia coli* and *Bacillus brevis* and variation as a function of growth phase, nitrogen source, and C: N ratio. *Colloids Surf B Biointerfaces*. 2006; 50(2):112–119.
60. Fatima Hamadi, Hassan Latrache, Hafida Zahir, Soumaya El Abed, Mostafa Ellouali, Ibsouda Koraichi Saad. The Relation Between the Surface Chemical Composition of *Escherichia coli* and their Electron Donor/Electron Acceptor (Acide-base) Properties. *Res J Microbiol*. 2012; 7(1):32–40.
61. Terada A, Yuasa A, Kushimoto T, Tsuneda S, Katakai A, Tamada M. Bacterial adhesion to and viability on positively charged polymer surfaces. *Microbiology*. 2006; 152(12):3575–3583.
62. Qi Y, Ma HL, Du ZH, Yang B, Wu J, Wang R, Zhang XQ. Hydrophilic and Antibacterial Modification of Poly(lactic acid) Films by γ -ray Irradiation. *ACS Omega*. 2019; 4(25):21439–21445.
63. Popelka A, Abdulkareem A, Mahmoud AA, Nassr MG, Al-Ruweidi MKAA, Mohamoud KJ, Hussein MK, Lehocky M, Vesela D, Humpolíček P, Kasak P. Antimicrobial modification of PLA scaffolds with ascorbic and fumaric acids via plasma treatment. *Surf Coat Technol*. 2020; 400:126216.

64. Robert N. Wenzel. Theory of Wetting Action at Solid Surfaces. *Ind Eng Chem*. 1943; 28(8):988–994.
65. Alakrach AM, Noriman NZ, Dahham OS, Hamzah R, Alsaadi MA, Shayfull Z, Syed Idrus SZ. *J Phys Conf Ser*. 2018; 1019(1):12065.
66. Luque-Agudo V, Romero-Guzmán D, Fernández-Grajera M, González-Martín L, Gallardo-Moreno AM. Ageing of solvent-casting PLA-Mg hydrophobic films: Impact on bacterial adhesion and viability. *Coatings*. 2019; 9(12):814.
67. Dabbaghi A, Kabiri K, Ramazani A, Zohuriaan-Mehr MJ, Jahandideh A. Synthesis of bio-based internal and external cross-linkers based on tannic acid for preparation of antibacterial superabsorbents. *Polym Adv Technol*. 2019; 30(11):2894–2905.
68. Xu G, Liu P, Pranantyo D, Neoh KG, Kang ET, Lay-Ming Teo S. One-Step Anchoring of Tannic Acid-Scaffolded Bifunctional Coatings of Antifouling and Antimicrobial Polymer Brushes. *ACS Sustain Chem Eng*. 2019; 7(1):1786–1795.
69. Kahkeshani N, Farzaei F, Fotouhi M, Alavi SS, Bahramsoltani R, Naseri R, Momtaz S, Abbasabadi Z, Rahimi R, Farzaei MH, Bishayee A. Pharmacological effects of gallic acid in health and disease: A mechanistic review. *Iran J Basic Med Sci*. 2019; 22(3):225–237.
70. Balouiri M, Bouhdid S, Sadiki M, Ouedrhiri W, Barkai H, El Farricha O, Ibsouda SK, Harki EH. Effect of preconditioning cobalt and nickel-based dental alloys with *Bacillus* sp. extract on their surface physicochemical properties and theoretical prediction of *Candida albicans* adhesion. *Mater Sci Eng C*. 2017; 71:111–117.
71. Olewnik-Kruszkowska E, Gierszewska M, Jakubowska E, Tarach I, Sedlarik V, Pummerova M. Antibacterial films based on PVA and PVA-chitosan modified with poly(hexamethylene guanidine). *Polymers*. 2019; 11(12):2093.
72. Van Loosdrecht MCM, Lyklema J, Norde W, Schraa G, Zehnder' AJB. The Role of Bacterial Cell Wall Hydrophobicity in Adhesion. *Appl Environ Microbiol*. 1987; 53(8):1893–1897.
73. Zheng S, Bawazir M, Dhall A, Kim HE, He L, Heo J, Hwang G. Implication of Surface Properties, Bacterial Motility, and Hydrodynamic Conditions on Bacterial Surface Sensing and Their Initial Adhesion. *Front Bioeng Biotechnol*. 2021; 9:643722.
74. Ozkan E, Mondal A, Singha P, Douglass M, Hopkins SP, Devine R, Garren M, Manuel J, Warnock J, Handa H. Fabrication of Bacteria- And Blood-Repellent Superhydrophobic Polyurethane Sponge Materials. *ACS Appl Mater Interfaces*. 2020; 12(46):51160–51173.
75. Naderizadeh S, Dante S, Picone P, Di Carlo M, Carzino R, Athanassiou A, Bayer IS. Bioresin-based superhydrophobic coatings with reduced bacterial adhesion. *J Colloid Interface Sci*. 2020; 574:20–32.
76. Montgomerie Z, Popat KC. Improved hemocompatibility and reduced bacterial adhesion on superhydrophobic titania nanoflower surfaces. *Mater Sci Eng C*. 2021; 119:111503.
77. Qin XH, Senturk B, Valentin J, Malheiro V, Fortunato G, Ren Q, Rottmar M, Maniura-Weber K. Cell-Membrane-Inspired Silicone Interfaces that Mitigate Proinflammatory Macrophage Activation and Bacterial Adhesion. *Langmuir*. 2019; 35(5):1882–1894.
78. Moazzam P, Razmjou A, Golabi M, Shokri D, Landarani-Isfahani A. Investigating the BSA protein adsorption and bacterial adhesion of Al-alloy surfaces after creating a hierarchical (micro/nano) superhydrophobic structure. *J Biomed Mater Res A*. 2016; 104(9):2220–2233.
79. Tsibouklis J, Stone M, Thorpe AA, Graham P, Peters V, Heerlien R, Smith JR, Green KL, Nevell TG. Preventing bacterial adhesion onto surfaces: The low-surface-energy approach. *Biomaterials*. 1999; 20(13):1229–1235.
80. Genzer J, Efimenko K. Recent developments in superhydrophobic surfaces and their relevance to marine fouling: A review. *Biofouling*. 2006; 22(5):339–360.